JOURNAL OF MATERIALS SCIENCE 31 (1996) 2609–2613

Effect of annealing on the structure and electrical properties of sulfur-doped amorphous c-BN layers

J. SZMIDT, A. WERBOWY, L. JARZĘBOWSKI, T. GEBICKI*
*Institute of Microelectronics and Optoelectronics, and *Institute of Physics, Warsaw University of Technology, Koszykowa 75, 00-662 Warsaw, Poland*
I. PETRAKOVA
Mendeleev's University of Chemistry and Technology of Russia, Minsskaya Sq. 9, 125047 Moscow, Russia
A. SOKOŁOWSKA, A. OLSZYNA
Institute of Materials Science and Engineering, Warsaw University of Technology, Narbutta 85, 02-524 Warsaw, Poland

Undoped and sulfur doped amorphous cubic boron nitride (a-cBN) layers were deposited on to silicon substrates by reactive pulse plasma (RPP) method. Subsequently they were annealed at 475, 500 and 700 K for 1 h in pure nitrogen atmosphere. In this study structural and electronic properties of unannealed and annealed layers were investigated. The results show that a consequence of annealing is formation of microstructural stable nanocrystalline cubic boron nitride film as well as substitutional location of introduced *in situ* donor impurities. This resulted in creation of a-cBN(n-type)–Si(p-type) heterojunction.

1. Introduction

Diamond-like BN (c-BN) layers can be produced under thermodynamic non-equilibrium conditions by ion-beam [1, 2], high-frequency or microwave plasma (enhanced by electron thermionic emission and substrate biasing) [3–6] as well as pulse plasma [7] methods. Such layers, deposited on to unheated substrates are amorphous or nanocrystalline and are often composed of stable, i.e. h-BN as well as unstable (high-pressure) c-BN forms. It seems that amorphous c-BN (a-cBN) films are more suitable for electronic applications than amorphous diamond-like carbon (DLC) films. This is because of the fact that the presence in the former ones of h-BN phase does not result in undesirable leakage currents, which show up in the amorphous diamond when it contains a graphite component. The aim of this study was to examine if it would be possible to optimize electrical parameters of a-cBN layers when their structure is influenced by the annealing process carried out at the lowest possible temperature. In our previous study [8], on the basis of obtained current–voltage characteristics, we found that sulfur-containing 1000 nm thick a-cBN layers became n-type semiconductors after annealing at 600 K. In this paper we present the results of our recent studies on the impact of annealing on changes in the properties of thinner (500 nm thick) a-cBN films. The smaller thickness was chosen in order to enable more detailed structural investigations, especially electron diffraction measurements of produced layers.

2. Experimental procedure

500 nm thick a-cBN layers were deposited on to silicon (p-type, $\rho \approx 15\ \Omega$ cm and n-type, $\rho \approx 3$–$4\ \Omega$ cm) substrates by the reactive pulse plasma method (RPP), described earlier [7]. Layers were *in situ* doped by sulfur atoms in order to obtain the n-type semiconducting material. The sulfur concentration was determined by X-ray microprobe (Cameca 30 Semiprobe). A schematic diagram of the plasma-assisted chemical vapour deposition (PACVD) apparatus is shown in Fig. 1 while deposition process parameters are given in Table I. Layers were annealed at 475, 500 and 700 K for 1 h in a pure nitrogen atmosphere in a clean-room of the 1000 cleanness class. Thicknesses of the layers, X_i, as well as their refractory indexes, n, were evaluated by ellipsometry (Gaertner 117, $\lambda = 234.8$ nm). Phase composition and microstructure were studied by Raman microspectrometry (Dilor XY-800, $\lambda = 234.8$ nm) as well as electron diffraction (transmission electron microscope JEM100B). In order to examine the electrical properties of the produced layers, the metal (aluminium and gold) dot contacts were evaporated on top of them. As a result, metal-layer–semiconductor structures were obtained, allowing subsequent current–voltage (I–V)

0022–2461 © *1996 Chapman & Hall*

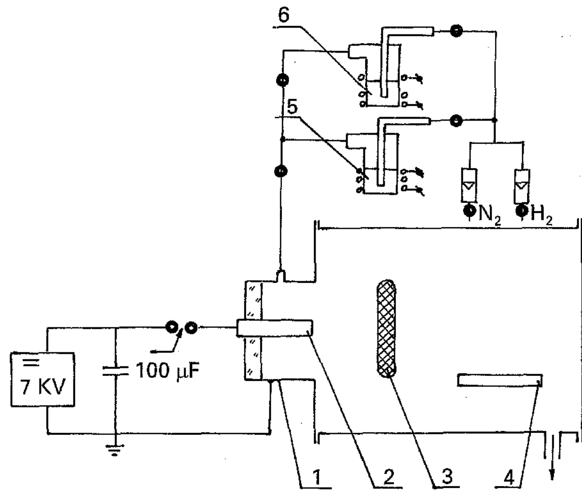

Figure 1 A schematic diagram of the PACVD apparatus 1, external water-cooled electrode; 2, internal electrode (graphite coated with a pyrographite layer; 3, plasma packet; 4, substrate; 5, saturator ($BH_3{\cdot}NH_3$); 6, saturator (S).

TABLE I Deposition parameters

Reactant gas	$BH_3{\cdot}NH_3$
Carrier gas	N_2–H_2 (1:1)
Pressure (hPa)	~ 0.1
Energy dissipated per pulse (kJ)	0.8
Substrate temperature (K)	300

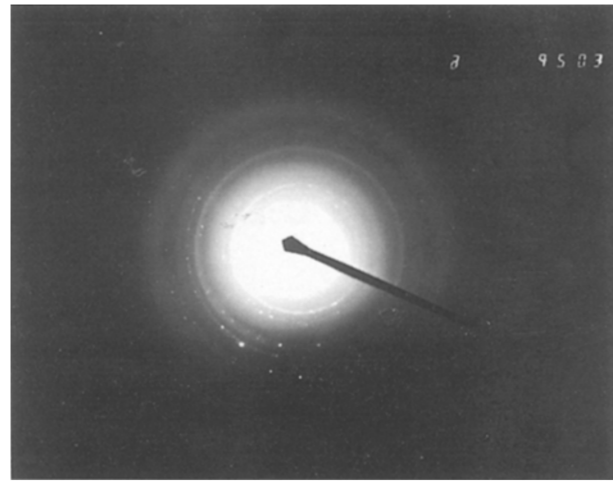

Figure 2 Electron diffraction pattern of an unannealed BN layer.

TABLE II Interplanar distances of unannealed layers

d_{exp} (nm)	d E–BN (nm) (ASTM card 18251)
0.294	0.298
0.199	0.195
0.168	0.170
0.142	0.140
0.122	0.125

and high-frequency (1 MHZ) capacitance–voltage (C–V) measurements to be made.

3. Results

The sulfur concentration in the deposited layers (all approximately 0.5 μm thick), as determined by X-ray microprobe, did not exceed 2000 p.p.m.

3.1. Unannealed layers

As deposited, the obtained layers were partly nanocrystalline and partly amorphous. The nanocrystalline compound was composed of E–BN phase, as shown in the electron diffraction data (Fig. 2 and Table II) and by the peak in the Raman spectrum at 1580 cm^{-1} (not previously reported, Fig. 3). The amorphous component manifested itself in the Raman spectrum by a broad peak observed near 1360 cm^{-1}, which might correspond to the mixture of h-BN and c-BN phases. However, their unequivocal identification by the Raman scattering method was not possible. Results of all structural investigations are given in Table III.

Electrical properties of undoped a-cBN layers were studied earlier and reported elsewhere [9–11]. I–V characteristics of sulfur-doped and undoped layers were either symmetrical or showed an asymmetrical character, uncharacteristic for a diode, reflecting only the silicon substrate's state changes under the bias applied [9]. Analysis of the accumulated curves indicates current flow mechanisms typical for insulators (Frenkel–Poole or TAT) [9, 10]. Similarly, the high-frequency C–V curves are characteristic for MIS

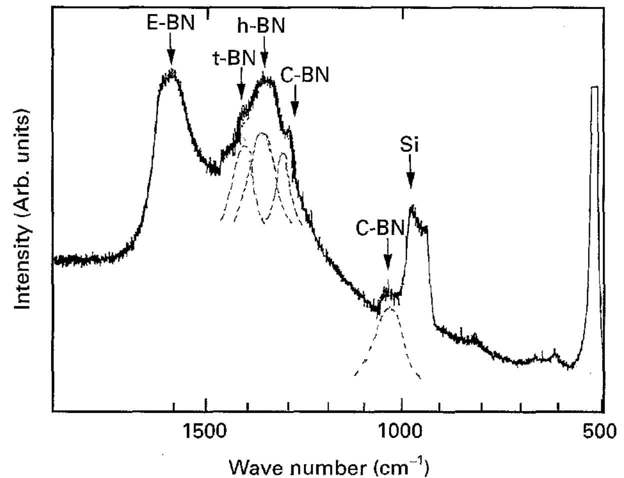

Figure 3 Raman spectrogram of an unannealed BN layer.

structure with an aBN layer as an insulator [9, 10]. In particular, it is very interesting that sulfur doping did not affect in any appreciable way either the form of the I–V or the C–V characteristics.

3.2. Annealed layers

After annealing at temperatures higher than 500 K the properties of the obtained a-cBN layers were distinctly changed. Their microstructure became completely nanocrystalline. The shape of the electron diffraction patterns (Fig. 4, Table IV) as well as the presence of very broad, yet separate, peaks in the Raman spectrum (Fig. 5) seem to be evidence that the amorphous phase disappeared in the investigated BN

TABLE III BN forms identified from Raman spectra

	Raman shift peak (cm^{-1})		
	Observed	Identified BN form	Remarks
Unannealed	1570	E-BN after TEM	High
	1360	t-BN after IR: 1425 cm^{-1} [13]	Very broad
		h-BN 1366 cm^{-1} [14]	
		c-BN 1304 cm^{-1} [15]	
	1056	c-BN [15]	Very small
Annealed	1570	E-BN after TEM	Narrow
		t-BN after IR [13]	–
	1367	h-BN [14]	–
	1304	c-BN [15]	–
	1056	c-BN [15]	–
	805	t-BN after IR	High

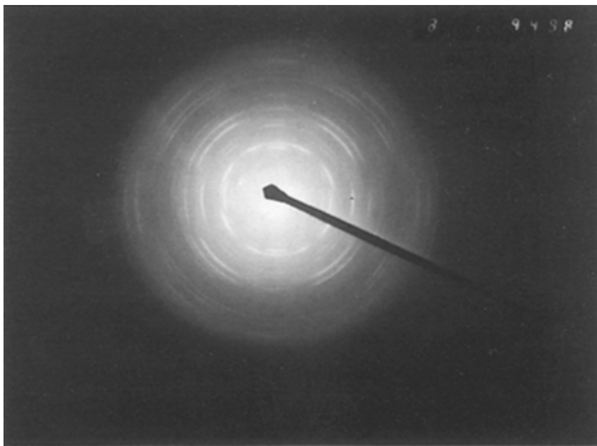

Figure 4 Electron diffraction pattern of an annealed BN layer.

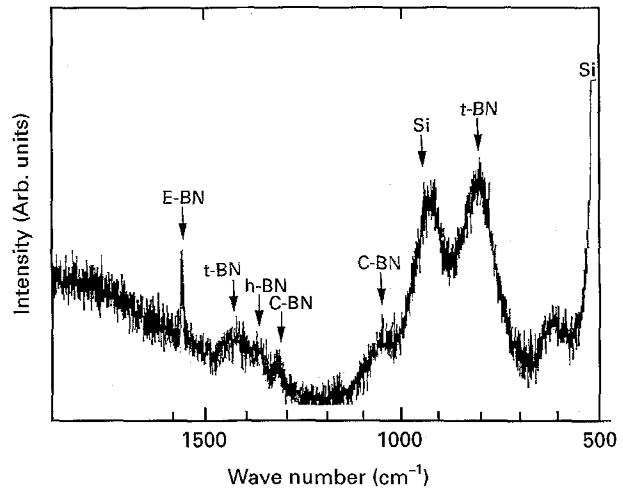

Figure 5 Raman spectrogram of an annealed BN layer.

TABLE IV Interplanar distances of annealed layers

d_{exp}(nm)	d E–BN (nm) (ASTM card 18251)
0.296	0.298
0.215	0.210
0.174	0.170
0.158	0.154
0.130	0.135
0.107	–
0.102	–

layers. In general, the following allotropic forms of boron nitride were identified to be present in these layers: E-BN, c-BN, h-BN and t-BN. The phase identification of material is shown in Table III.

The electrical properties of undoped layers did not change as a result of annealing. More detailed analysis of the influence of the annealing process on their properties can be found elsewhere [12].

A completely different situation existed in the case of the electrical properties of structures made of aBN layers doped with sulfur (dBN), as they became semiconducting after annealing. Typical I–V and high-frequency C–V characteristics of Au–BN(n)–Si(p) structures are shown in Fig. 6. It can be seen that especially the I–V characteristics of samples with gold contacts became diode-like, with the forward ($U < 0$) current approximately two orders of magnitude greater, compared to unannealed structures. A similar tendency was observed for the I–V curves of samples with aluminium contacts, where the rise in current in the forward direction was also noticeable, although not so high. However, it is also notable that the characteristics of different samples are considerably scattered and also show instabilities.

The C–V curves of annealed structures show typical diode-like behaviour and are also unstable, similar to the discussed I–V characteristics of the samples with aluminium metallization (Fig. 6b). These results confirm our previous findings concerning thicker films, presented elsewhere [8].

4. Discussion

Our investigations show that thermally activated processes have an evident impact on the microstructural changes of BN layers, as well as on their semiconducting properties. After annealing, without any noticeable transformation of their nanocrystalline structure, they show an increase in the short-range matrix order, because the separate BN forms become distinguishable in measured Raman spectra, as well as furnishing evidence that the amorphous phase apparently disappears. In as-deposited as well as in annealed layers,

10^{-3} I (A)
10^{-4}
10^{-5}
10^{-6}
10^{-7}
10^{-8}
10^{-9}
10^{-10}
−40 −30 −20 −10 0 10 20 30 40
(a)
V (V)

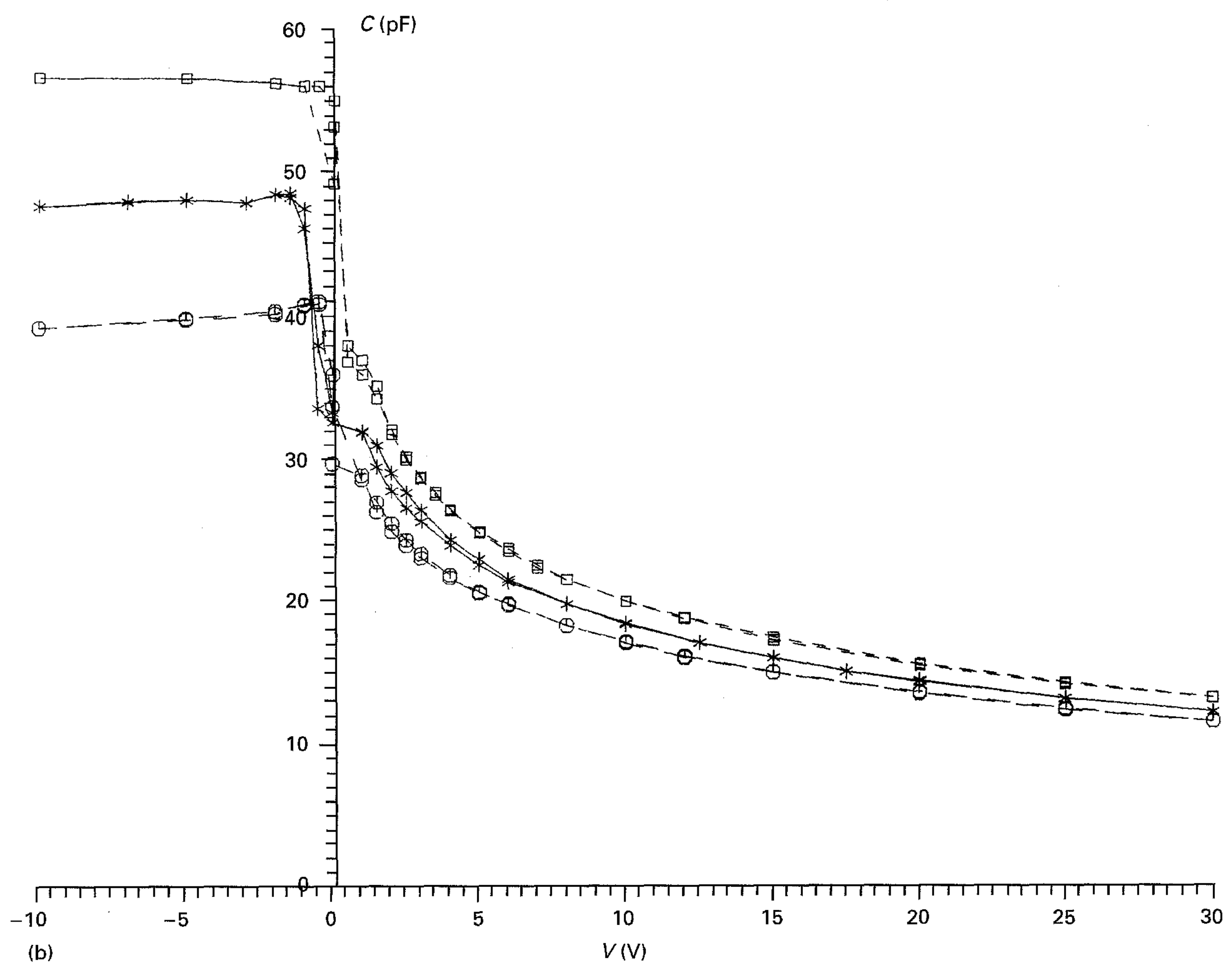

Figure 6 Electrical characteristics of annealed Au–BN(n)–Si(p) structures: (a) I–V curves; (b) C–V curves.

electron diffraction patterns always reveal only the presence of the E-BN form, which leads to the conclusion that this form constitutes the main component of the ultrafine grained part of the material. It is possible that h-BN and c-BN forms might exist side by side in the amorphous component of unannealed layers, subsequently crystallizing when higher temperatures were applied. The t-BN form, however, appeared only after the annealing process. It can be assumed that it originates from the h-BN form, which transformed into the t-BN form at the time of annealing, under the mechanical stress conditions accompanying the crystallization process.

Nevertheless, the most important change in the properties of the layers resulting from annealing is the formation of the monopolar semiconductor [8]. This shows that aBN films produced by the RPP method can be effectively doped *in situ* by sulfur atoms, subsequently forming with the silicon (after thermal treatment) a heterojunction, for example the BN(n)–Si(p). It seems that sulfur atoms, introduced *in situ* into the layers initially become interstitials in the random matrix of unannealed material. Annealing, however, makes them move to the substitutional locations, which results in the creation of donor levels in the forbidden gap of BN.

The most probable process responsible for the described changes in structure and properties resulting from sulfur atom relocation, seems to be diffusion.

5. Conclusion

Our investigations show that low-temperature diffusion, which takes place in nanocrystalline–amorphous BN layers obtained by a pulse plasma method, results in substitutional location of introduced *in situ* donor impurities. It also affects the formation of the stable microstructure of these layers without unbalancing the metastable BN phase stability. Application of an annealing process allows the nanocrystalline cubic BN *n*-type film to be obtained, which is the first step towards the fabrication of diodes with the use of a-cBN layers.

Acknowledgements

This work was supported by grants 503/904 from Warsaw University of Technology and 3.3602.91.02 from the Polish State Committee for Scientific Research.

References

1. S. SHANFIELD and R. WOLFSON, *J. Vac. Sci. Technol.* **A1** (1983) 323.
2. M. SATOU and F. FUJIMOTO, *Jpn J. Appl. Phys.* **22** (1983) L171.
3. K. INAGAWA, K. WATANABE, H. OHSONE, H. SAITOH and A. ITOH, *J. Vac. Sci. Technol.* **A5** (1987) 2696.
4. D. J. KESTER and R. MESSIER, *J. Appl. Phys.* **72** (1992) 504.
5. D. C. CAMERON, M. Z. KARIM and M. S. J. HASHMI, *T.S.F.* **236** (1993) 96.
6. H. SAITOH and W. A. YARBROUGH, *Diam. Rel. Matter.* **1** (1992) 137.
7. M. SOKOŁOWSKI, A. SOKOŁOWSKA, Z. ROMANOWSKI, B. GOKIELI, M. GAJEWSKA, *J. Cryst. Growth* **52** (1981) 165.
8. J. SZMIDT, A. WERBOWY, A. MICHALSKI, A. OLSZYNA, A. SOKOŁOWSKA and S. MITURA, *Diam. Rel. Matter* **4** (1995) 1131.
9. J. SZMIDT, A. JAKUBOWSKI, A. MICHALSKI and A. RUSEK, *T.S.F.* **110** (1983) 7.
10. J. SZMIDT, *Diam. Rel. Matter* **1** (1992) 681.
11. T. BROŻEK, J. SZMIDT, A. JAKUBOWSKI and A. OLSZYNA, *ibid.* **3** (1994) 720.
12. J. SZMIDT, A. JAKUBOWSKI and A. BALASIŃSKI, *T.S.F.* **142** (1986) 269.
13. H. SAITOH, T. HIROSE, T. OHTSUKA and Y. ICHINOSE, *Appl. Phys. Lett.* **13** (1994) 1638.
14. R. J. NEMANICH, S. A. SOLIN and R. M. MARTIN, *Phys. Rev.* **23** (1981) 6348.
15. O. BRAFMANN, G. LENGYEL, S. S. MITRA, P. J. GIELISSE, J. N. PLENDL and L. C. MANSON, *Solid State Commun.* **6** (1968) 523.

Received 25 April
and accepted 23 November 1995